

October 5, 1995

Pion Irradiation Studies of CVD Diamond Detectors

C. Bauer¹, I. Baumann¹, C. Colledani², J. Conway³, P. Delpierre⁴, F. Djama²,
W. Dulinski², A. Fallou⁴, K.K. Gan⁵, R.S. Gilmore⁶, E. Grigoriev⁴, G. Hallowell⁴,
S. Han⁷, T. Hessing⁸, J. Hrubec⁹, D. Husson², H. Kagan⁵, D. Kania¹⁰, R. Kass⁵,
K.T. Knöpfle¹, M. Krammer⁹, T.J. Llewellyn⁶, P.F. Manfredi¹¹, L.S. Pan¹²,
H. Pernegger⁹, M. Pernicka⁹, V. Re¹¹, S. Roe⁸, D. Roff⁶, A. Rudge⁸,
M. Schaeffer², S. Schnetzer³, V. Speziali¹¹, R. Stone³, R.J. Tapper⁶,
R. Tesarek³, W. Trischuk⁸, R. Turchetta², G.B. Thomson³,
R. Wagner⁷, P. Weilhammer⁸, C. White⁵,
S. Zhao⁵, H. Ziock⁷, M.M. Zoeller⁵

Abstract

We report here the results of a test to ascertain the radiation hardness properties of CVD diamond detectors to 300 MeV/c pions. In this test, CVD diamond detectors were exposed to 8×10^{13} pions per cm² using the high intensity pion beam at the Paul Scherrer Institut. For comparison, silicon photodiodes were exposed to similar fluences at the same time. The measurements and the dosimetry during the irradiations are described herein. As expected, the silicon devices degraded. The diamond devices showed no degradation in collected charge and no increase in leakage current.

1 MPI-Heidelberg, D69029 Heidelberg, Germany

2 LEPSI, CRN Strasbourg 67037, France

3 Rutgers University, Piscataway, NJ 08855, U.S.A.

4 CPPM, Marseille 13288, France

5 The Ohio State University, Columbus, OH 43210, U.S.A.

6 Bristol University, Bristol BS8 1TL, England

7 Los Alamos National Laboratory, Los Alamos, NM 87545, U.S.A.

8 CERN, CH-1211, Geneva 23, Switzerland

9 Institut für Hochenergiephysik der Österr. Akademie d. Wissenschaften, A-1050 Vienna, Austria

10 Lawrence Livermore National Laboratory, Livermore, CA 94550, U.S.A.

11 Università di Pavia, Dipartimento di Elettronica, 27100 Pavia, Italy

12 Sandia National Laboratory, Livermore, CA 94550, U.S.A.

Submitted to Nuclear Instruments and Methods A.

1 Introduction

One of the attractive features of diamond charged particle detectors for high luminosity particle physics applications is their expected radiation hardness. Very near an interaction region in the LHC, at radii smaller than 15 cm, the predominant source of radiation is charged pions [1, 2]. During the lifetime of the LHC it is expected that a detector located 6 cm from the interaction region will receive fluences of approximately 10^{15} pions per cm^2 . Furthermore a large fraction of these pions will have very low momenta (coming from the hadronization of jets) and thus can excite nuclear resonances in the detector material.

Previous irradiation studies of diamond detectors with alpha particles, ^{60}Co photons, and ^{90}Sr electrons indicate that CVD diamond is extremely radiation resistant to these sources [3, 4, 5]. That work reported, however, a curious effect: at low doses of photons or electrons (less than 0.1 kGy) the observed charge signal increases with dose. Although not fully understood, the working hypothesis is that ionisation from the irradiation fills trapping centers in the diamond, allowing electrons and holes to move farther, giving rise to an increase in the observed signal size. In an attempt to extend the experimental information on the radiation hardness of CVD diamond, a set of 3 diamond detectors [6] was exposed to a 300 MeV/c pion beam at the Paul Scherrer Institut (PSI) in June of 1994. Pions are expected to cause more displacement damage than either photons or electrons and hence provide additional information. The diamond devices were made from the same wafer used for the photon irradiation reported earlier. The samples were characterized before and after the irradiation. During the irradiation the beam-induced current was monitored.

In this paper, we describe the irradiation procedure and the dosimetry used to quantify the doses received. We also describe the collection distance measurements performed before and after irradiation as tests for possible damage. Having no evidence for degradation at the doses reported, we comment on the feasibility of extending this study to higher doses.

2 Irradiations and Dosimetry

The samples were exposed in the πE1 beam at PSI near Villigen in Switzerland. The momentum of the pion beam was tuneable up to 400 MeV/c. The beam momentum for the work reported here was 300 MeV/c with a 10% momentum spread. This pion momentum was chosen since it corresponds to the peak of the pion-nucleon cross-section. The πE1 beam line was designed to deliver high pion fluences. Protons were eliminated from the beam with a final focus, which caused the typical proton momenta from the source to be focused upstream of the samples being irradiated. A series of carbon filters effectively removed the high energy protons which were still able to penetrate downstream on the beam axis. The proton flux was measured to be less than 2% of the total. Neutrons were removed from the beam with a dog-leg in the beam line upstream of the samples under test. The electron and muon contaminations were measured to be less than 5% and 10% respectively.

The detectors irradiated during this test were attached to 35 mm slide mounts and placed in a slide tray for easy placement and removal. The slide tray was mounted inside the sample holder shown in Fig. 1. The pion beam spot size was 19 mm (σ) at the entrance of the slide tray and thus completely irradiated the test samples. The pion fluence at various points in the sample holder volume was measured with $1 \times 1 \text{ cm}^2$ aluminum foils. The aluminium foils were placed throughout the sample holder volume – a length of 25 cm along the beam line and an area of $1 \times 1 \text{ cm}^2$ perpendicular to the beam. The exposure of aluminum to pions produces a known amount of ^{24}Na . After exposure, the calibration foils were monitored in a gamma spectrometer to determine the amount of ^{24}Na induced. With the known Al to

Sample	A	B	C
Serial Number	P5	U3	U4
Area (cm ²)	0.42	0.60	0.33
Thickness (μm)	260	430	430
Contact diameter (cm)	0.39	0.50	0.33
Contact metallization	Cr/Au	Cr/Au	Cr/Au

Table 1: Mechanical properties of the diamond detectors.

Na transmutation cross-section it is then possible to determine the pion fluence. The total fluence varied by a factor of three along the beam within the sample holder volume.

The pion flux was cross-calibrated to the current in an ionisation chamber which gave a measure of the relative flux over the course of the irradiation. This in turn was related to the beam-induced current both in the silicon and diamond structures under study. In fact, the constancy of the ratio of the diamond beam-induced current to the beam flux make them ideal for beam intensity monitors in future tests of this kind.

3 Diamond Signal Characterization

The diamond samples studied here were cut from a single wafer. In Table 1 we show the mechanical properties of the three diamonds used. Two of the samples were unpolished (B, C), and one was polished on both the growth and substrate side (A). Circular contacts were deposited on opposing surfaces of the diamond. The area of the contacts was made as large as possible on each detector for ease of use. A metallization of Chromium/Gold was used [7].

The diamond detectors were characterized before, during and after irradiation. The method used before and after consisted of measuring the charge collection distance, d , the mean distance averaged over the thickness of the material that an electron and hole move apart under the influence of an applied external field [7, 8] using a ⁹⁰Sr β -source. The collection distance is related to the sample thickness L , the charge generated in the material Q , the charge collected q , the average carrier mobility μ , the average carrier lifetime τ , and the applied electric field E , by

$$d = \mu E \tau = q \frac{L}{Q} \quad (1)$$

In Fig. 2 we show a schematic view of the source setup. Electrons from a 0.5 mCi ⁹⁰Sr source (maximum energy of 2.28 MeV) are used to excite the diamond detector after passing through a 2 mm diameter collimator. Events are triggered by a single scintillator indicating that the electron has passed through the diamond. The typical random singles rate of the scintillator is < 1 Hz while the typical event rate is 20-50 Hz. Events triggered in this manner detect electrons which deposit on average 8% more energy than minimum ionising particles.

In addition, the leakage current was measured before and after irradiation [9]. A typical I-V curve taken after the irradiation is shown in Fig. 3. The I-V characteristics may be used to infer problems in the contacts and changes in the bulk material. No such problems were observed here. The before and after I-V curves are consistent for all samples indicating no changes to the contacts and no increase in leakage current. The low leakage current observed is typical of detector grade diamond.

Sample	A, 2	B, 1	C
Fluence ($\times 10^{13}$ pions cm^{-2})	1.3	4.3	8.0
Time beam on (hours)	5.75	5.75	8.0
Temperature of irradiation ($^{\circ}\text{C}$)	27	27	5

Table 2: Exposure characteristics for the three diamond (A, B, C) and two silicon (1, 2) detectors used in this work.

Sample	A	B	2	1
Electrode area (cm^2)	0.12	0.20	0.25	0.25
Fluence ($\times 10^{13}$ pions cm^{-2})	1.3	4.3	1.3	4.3
Leakage current initial (nA at 100V)	0.0014	0.0011	25	25
Leakage current final (nA at 100V)	0.0014	0.0011	4,000	10,000
Beam-induced current (nA at 100V)	72	110	238	550

Table 3: The leakage and beam-induced currents measured in the diamond (A, B) and silicon (1, 2) samples.

In Table 2 we show the characteristics of the exposure used for each of the three samples. Diamond samples A and B and silicon samples 1 and 2 were exposed together when the pion beam intensity was relatively low. Their placement within the sample holder determined the fluence (see Fig. 1). Sample C was exposed separately when the pion beam reached its highest intensity. The total error on the dosimetry is estimated to be $\pm 25\%$.

During the exposure, the beam-induced current was monitored using an high impedance electrometer [10]. The beam-induced current, i_{beam} , is related to the pion fluence f , and area over which charge is collected A , by

$$i_{beam} = \frac{dq}{dt} = \frac{\delta f}{\delta t} \cdot \frac{Q}{L} \cdot d \cdot A \quad (2)$$

The online detector currents for diamond and silicon detectors are shown in Fig. 4 and Fig. 5. These plots show the reverse bias current in the various devices over the last two thirds of the irradiation. Note the difference in the current scales between the diamond and silicon data. Two families of current measurements are apparent in each plot, those in the presence of beam (diamonds) and those from the residual ‘‘leakage’’ current in the devices (stars) when the beam was off. Throughout the run when the pion beam was present, there were two discrete and constant intensities depending on the primary proton beam current: full intensity and roughly 85% of full intensity. The fine structure when the beam was present is clearly evident in the diamond data. Moreover for constant pion beams, the constancy of the diamond current is taken as further evidence that the samples’ charge collection properties were unchanged over a wide range of doses. In the case of silicon the fine structure when the beam was present is not discernable. There is clear evidence of the increase of leakage current with dose and of the annealing that occurs when the beams were turned off. The difference between the two families of points (in Figs. 4 and 5) is taken as the beam-induced current reported in Table 3. The dominant errors are a 25% uncertainty in the absolute fluence, a 1 nA precision on the measured current, and a 10 nA accuracy on the current scale.

4 Results

In Fig. 6 we show the collection distance for sample C as a function of electric field measured before and after pion irradiation. The collection distance after irradiation has increased over the pre-irradiation value by a factor of 1.5-1.8 depending on the electric field. In Fig. 7 we show the relative collection distance at an electric field of 10 kV/cm, normalized to the unirradiated value, as a function of fluence. The data below a fluence of 10^{11} cm⁻² were taken with electrons from the source setup described earlier. The points at 1.3, 4.3 and 8×10^{13} cm⁻² were taken with 300 MeV/c pions. These data confirm the rise of collection distance with small dose observed previously [4, 5]. The constancy of the collection distance, the tracking of the beam-induced currents with the pion flux, and the constancy of the leakage current in diamond at these large fluences indicate the radiation hardness of CVD diamond. Moreover, diamond appears to operate as expected at 27°C.

The silicon photodiodes showed a dramatic increase in leakage current as a function of pion fluence. Comparing the increase in leakage current with that found in 20 keV photon irradiations [11] we conclude the primary cause of the increase of leakage current in silicon from 300 MeV/c pions is displacement damage. Using the observed change in leakage current we find a damage constant in silicon of 3.1×10^{-17} A/cm/incident 300 MeV/c pion at 27°C. This may be compared with the measured damage constant in silicon for 800 MeV protons of 4.9×10^{-17} A/cm/incident 800 MeV proton at 20°C [12, 13]. Scaling the damage constant for protons up to account for the 7°C temperature difference we find that in silicon 300 MeV/c pions have a damage constant approximately two and a half times smaller than 800 MeV protons.

5 Conclusions

The data presented above indicates that the presently available CVD diamond detectors are radiation hard up to pion fluences of 8×10^{13} cm⁻². No evidence for deterioration of the signal response of the diamond samples was found. This is a strong indication that diamond based detectors will be able to withstand the harsh environment of the LHC very near to the interaction region. We intend to pursue these measurements with higher quality CVD diamond material up to fluences comparable to the lifetime dose at the LHC in future measurements. We expect to reach pion fluences of 10^{15} per cm² during the next PSI run.

6 Acknowledgments

We would like to thank the RD20 collaboration who provided the silicon photodiodes and leakage current data shown here for comparison to diamond.

References

- [1] A. Chilingarov and S. Roe, *Radiation Damage Projections for Silicon*, ATLAS INDET-No. 31, November 1993.
- [2] A. Gorfine and G. Taylor, *Particle Fluxes and Damage to Silicon in the ATLAS Inner Detector*, ATLAS INDET-No. 30, November 1993.
- [3] M.H. Nazaré *et al.*, *Development of Diamond Tracking Detectors for High Luminosity Experiments at the LHC*, CERN/DRDC 94-21, DRDC-P56, May 1994.
- [4] S. Han *et al.*, *Recent Results on the Radiation Hardness of CVD Diamond Detectors*, in the Proceedings of DPF94, Santa Fe, NM, July 1994.
- [5] H. Pernegger *et al.*, *Radiation Hardness Studies of CVD Diamond Detectors*, in the Proceedings of the 1995 Vienna Wire Chamber Conference to appear in NIM.
- [6] The CVD diamond was provided by St. Gobain/Norton Diamond Film, Goddard Road, Northboro, MA 01532.
- [7] S. Zhao, *Characterization of the Electrical Properties of Polycrystalline Diamond Films*, Ph.D. Thesis, The Ohio State University (1994).
- [8] L.S. Pan *et al.*, J. Appl. Phys. **74** (1993) 1086.
- [9] The device used to measure the I-V characteristics before and after the exposure was a Keithley 617 Programmable Electrometer with a precision of 0.1 pA.
- [10] The electrometer used to monitor the current during the exposure was a ten channel Keithley 2001 Electrometer with a 1 nA precision.
- [11] In work performed for CLEO, 20 keV x-rays were used to irradiate 300 μm thick silicon detectors. The increase in leakage current was monitored. The damage was found to be primarily a surface effect characterized by a damage constant of 5 nA/cm²/kRad. (Jim Alexander, private communication).
- [12] F. Lemeilleur *et al.*, Nucl. Instr. and Meth. **A360** (1995) 438.
- [13] H. Ziock *et al.*, IEEE Trans. Nucl. Sci. **37** (1990) 1238.

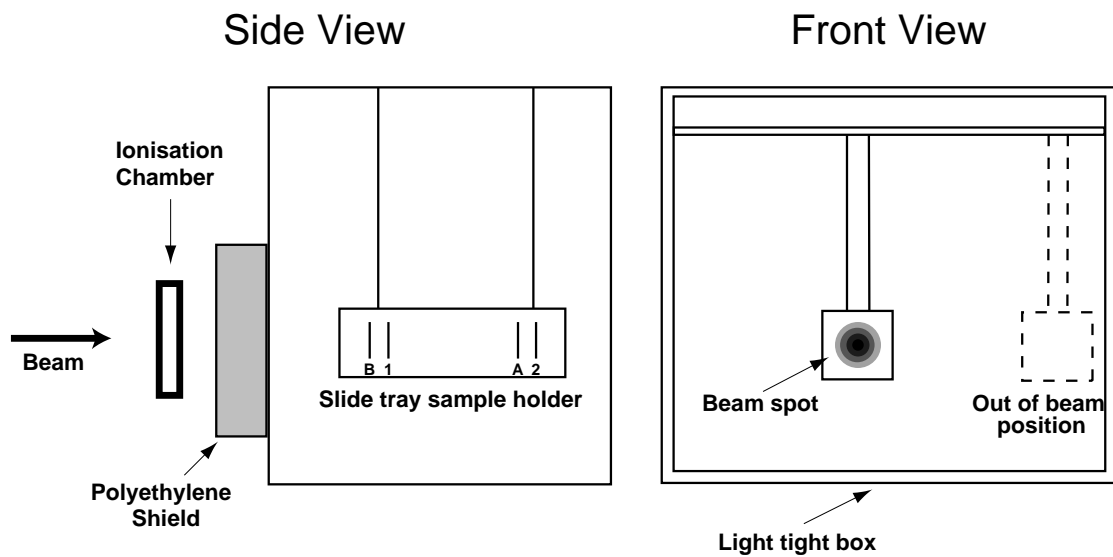


Figure 1: A schematic view of the PSI setup used to irradiate the diamond (A, B, C) and silicon (1, 2) samples. Samples A, B, 1, and 2 were exposed together. Samples A and 2 were placed at the low intensity position in the rear of the holder. Samples B and 1 were placed at the high intensity position in the front of the holder. Samples B and 1 obtained approximately three times the fluence of samples A and 2 for the same exposure time.

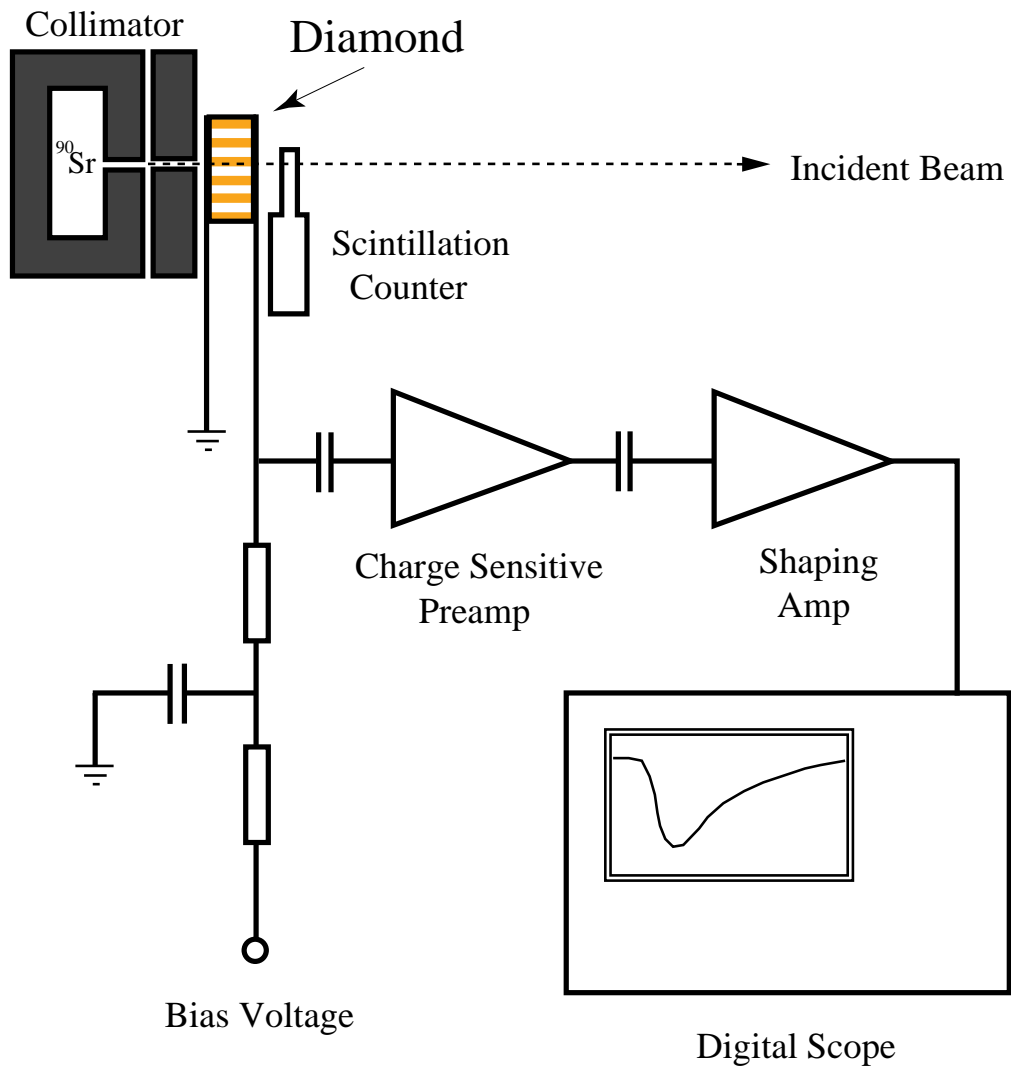


Figure 2: A schematic view of the source setup used to characterize the diamond samples.

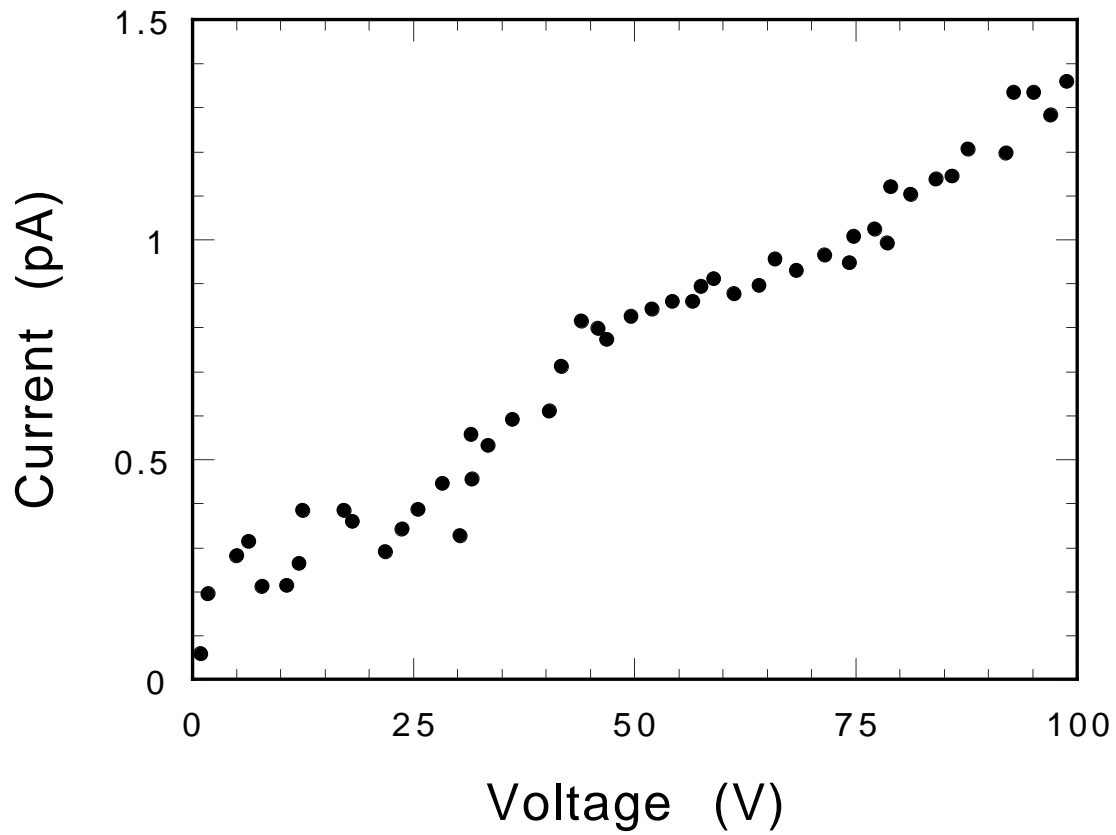


Figure 3: The I-V curve for sample A after irradiation.

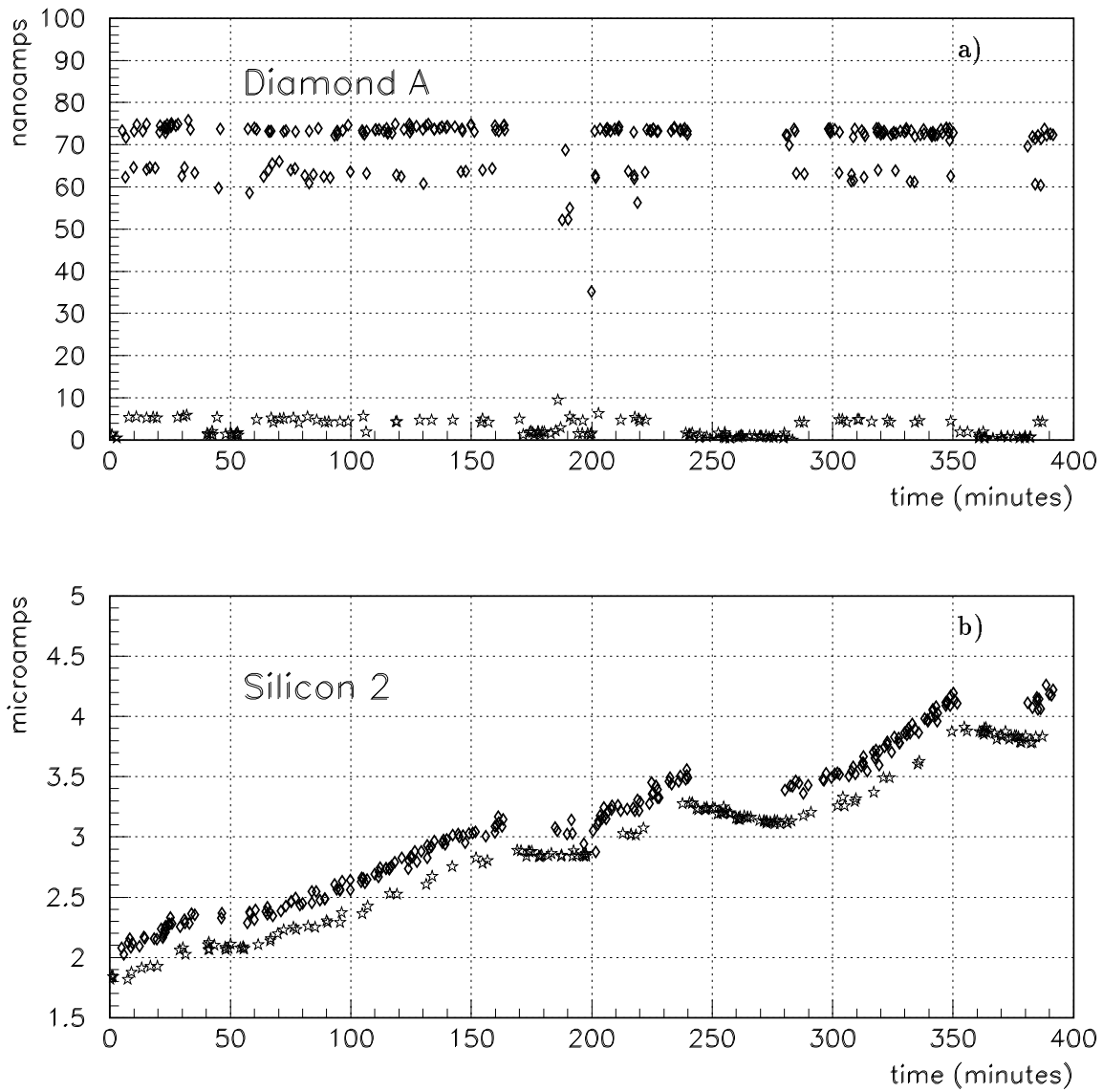


Figure 4: The online detector current in a) diamond sample A and b) silicon sample 2 in the low intensity (rear) position measured during the pion irradiation as a function of time. The time axis ($t = 0$) begins 200 minutes after the beginning of the irradiation. The pion fluence increases from 4×10^{12} pions/cm² at $t = 0$ to 1.4×10^{13} pions/cm² at $t = 400$ minutes in both graphs. The two families of points in each figure correspond to times when the beam was on (diamonds) and times when the beam was off (stars). During the data taking there were two intensities of running which are clearly identified in the diamond data. During the periods when the beam was off, the annealing effect in silicon is clearly evident. Note the difference in current scales between a) and b).

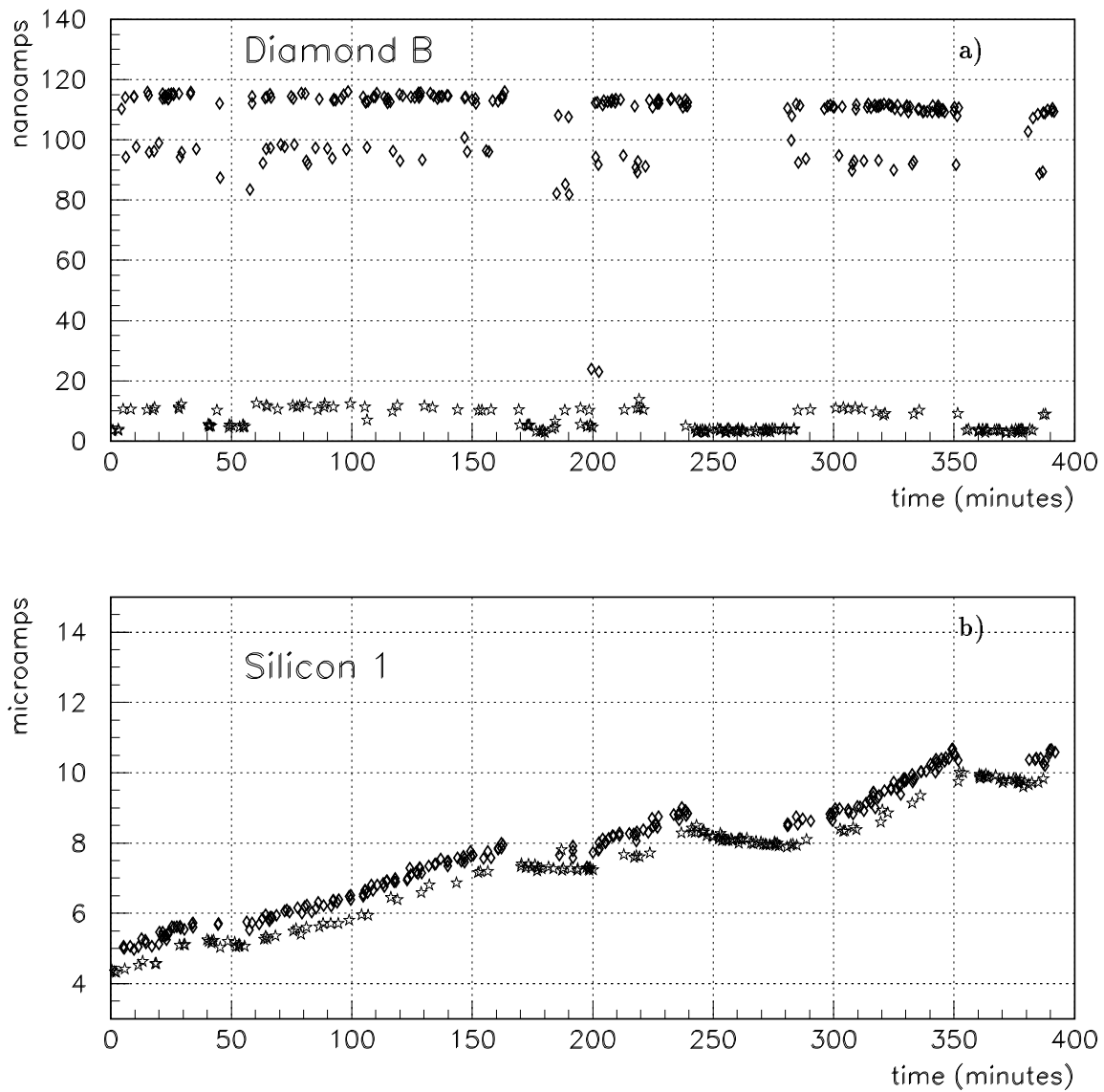


Figure 5: The online detector current in a) diamond sample B and b) silicon sample 1 in the high intensity (forward) position measured during the pion irradiation as a function of time. The time axis ($t = 0$) begins 200 minutes after the beginning of the irradiation. The pion fluence increases from 1.4×10^{13} pions/cm² at $t = 0$ to 4.3×10^{13} pions/cm² at $t = 400$ minutes in both graphs. Again the two families of points in each figure correspond to times when the beam was on (diamonds) and off (stars). The dominant effect in b) is the growth of the diode leakage current as the silicon is damaged.

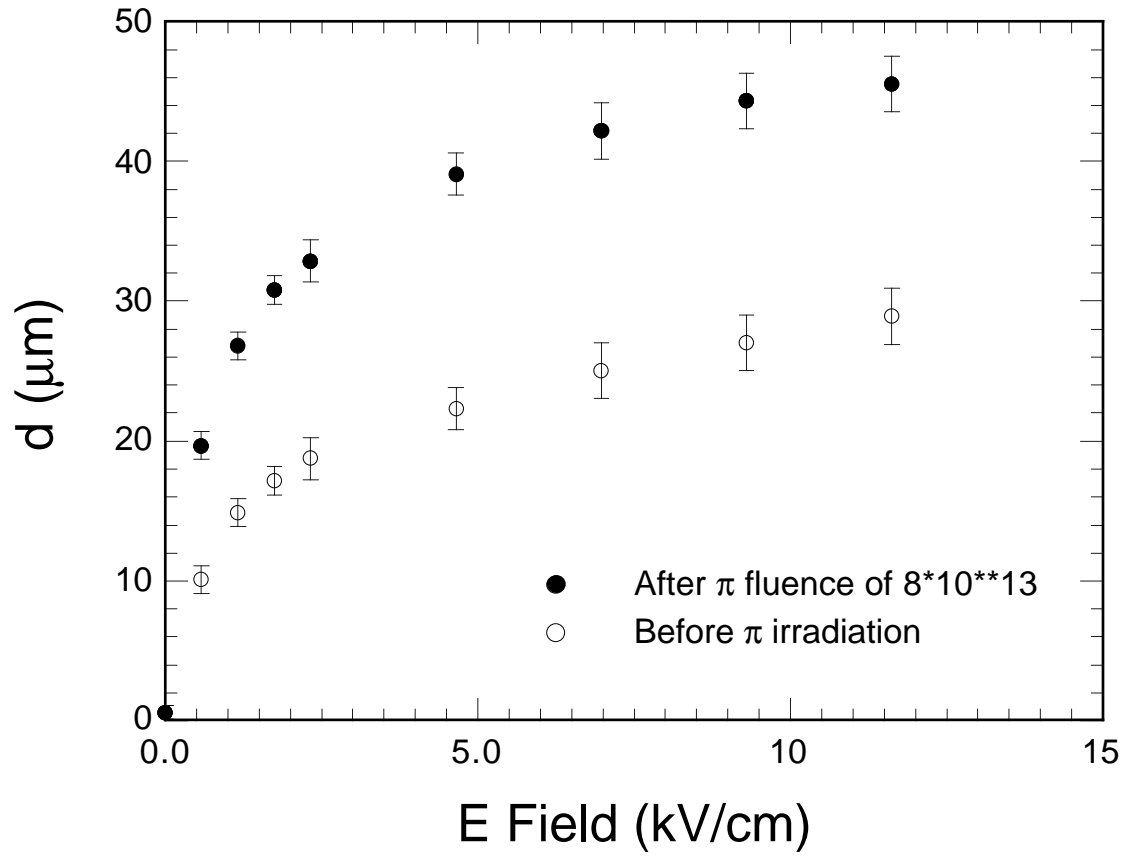


Figure 6: The collection distance as a function of electric field for sample C measured before and after pion irradiation.

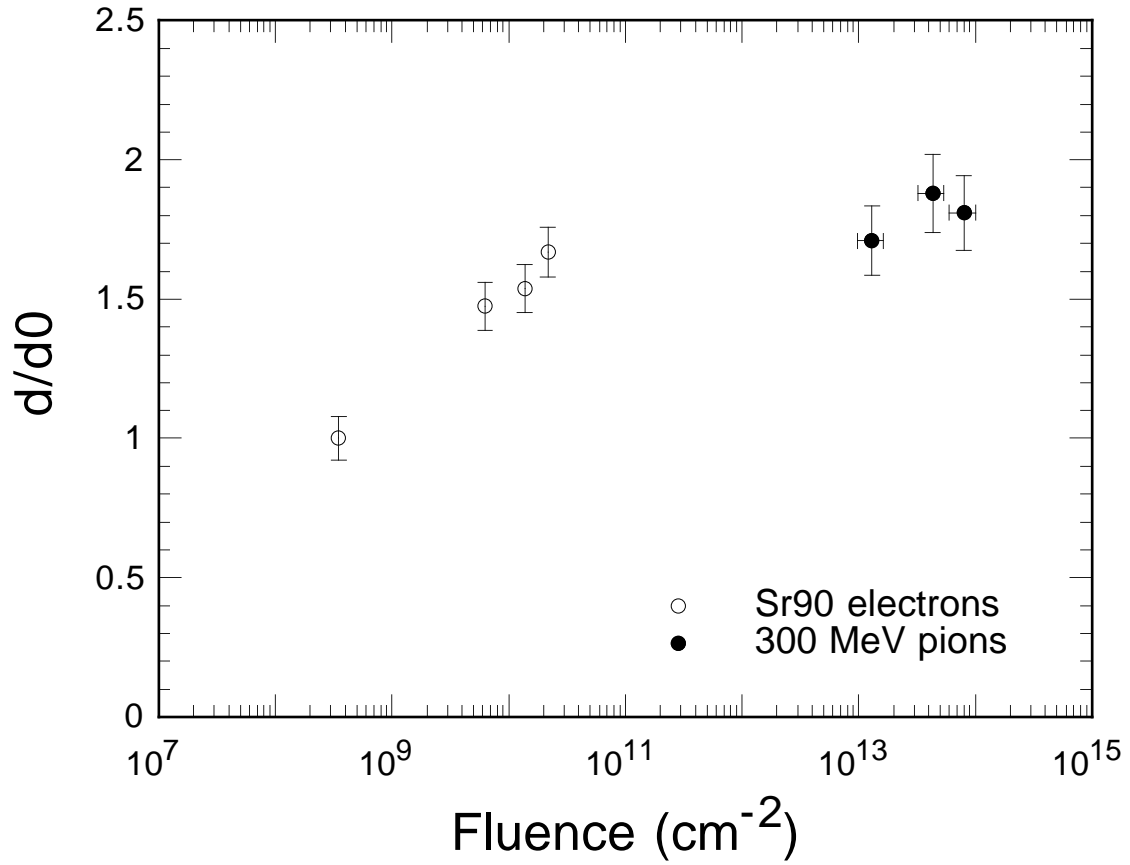


Figure 7: The relative collection distance (d/d_0) at an electric field of 10 kV/cm as a function of pion fluence normalized to the lowest fluence point.